Multipolar Ordering and Magnetization Reversal in Two-Dimensional Nanomagnet Arrays

E. Y. Vedmedenko,[1] N. Mikuszeit,[2] H. P. Oepen,[1] and R. Wiesendanger[1]
[1]*Institut für Angewandte Physik, Universität Hamburg, Jungiusstrasse 11a, 20355 Hamburg, Germany*
[2]*Universidad Autónoma de Madrid, E-28049 Spain*
(Received 7 February 2005; published 7 November 2005)

The low-temperature stable states and the magnetization reversal of realistic two-dimensional nanoarrays with higher-order magnetostatic interactions are studied theoretically. For a general calculus of the multipole-multipole interaction energy we introduce a Hamiltonian in spherical coordinates into the Monte Carlo scheme. We demonstrate that higher-order interactions considerably change the dipolar ground states of in-plane magnetized arrays favoring collinear configurations. The multipolar interactions lead to enhancement or decrease of the coercivity in arrays with in-plane or out-of-plane magnetization.

DOI: 10.1103/PhysRevLett.95.207202 PACS numbers: 75.75.+a, 75.10.−b, 75.60.Jk

Magnetic properties of artificially structured and self-organized magnetic media belong to the central questions of nanomagnetism as they give access to new phenomena that can be used in technology [1–3]. Magnetic memory applications require the increase of the density of dots per unit area, which is correlated with a decrease of dot diameter d and interdot distances R. Particles with lateral size smaller than the characteristic exchange length $d < \chi_{\mathrm{ex}}$ have a single domain magnetization configuration with a macroscopic magnetic moment. In densely packed systems these moments interact. The magnetostatic interaction is a crucial parameter as it determines the magnetization reversal. To identify the effects of the long-range interaction on magnetic behavior extensive experimental [2,4–9] and theoretical [10–12] studies of magnetic nanoarrays have been performed.

Experimental investigations show that in comparison with an infinite film, the interparticle interactions usually lead to a decrease of the switching field in patterned media with out-of-plane magnetization [2,5,7] and to an increase of the coercivity for in-plane magnetized particles [5,6,8,13]. Although in some cases an agreement of switching behavior with theoretical predictions has been obtained, it is often found that measured switching fields deviate significantly (10%–15%) from those expected from pure dipolar interactions ([5–7,9] and the references therein). The theory predicts a noncollinear antiferromagnetic ground state and weak coercivity for a square lattice, which comes close to the ideal situation of in-plane dipoles with zero in-plane self-coercivity [14,15], while experiments [6,13] reveal that patterning of a continuous film increases the coercivity considerably, e.g., $\mu_0 H_c$ goes from almost zero up to 22.8 mT for Co and 16 mT for NiFe arrays [6,13]. In addition, collinear magnetic superdomains in dense nanoarrays have been observed [16] instead of a noncollinear structure. In a triangular in-plane array a frustrated ferromagnetic state with closed loops and spirals has been predicted [11]. In the experiment, however, the vorticity was not observed and the coercivity exceeded that expected from the dipolar approximation [6,13]. A related nonsolved problem is the so-called superferromagnetism in two-dimensional nanoislands assemblies. Experimentally found superferromagnetic domains [9,17] lead to high coercivity, which is inconsistent with the strength of the dipolar coupling and the absence of the direct exchange interactions [9].

The quantitative disagreement between theory and experiment has been attributed to a variety of reasons as pinning of magnetization by structural inhomogeneities [6] or noncoherent rotation of magnetization [5,7]. Several investigations have been devoted to the question of how the dipolar interaction between the monodomain particles is modified by their finite size, i.e., the leading correction terms to the dipolar interaction have been determined [10,12]. The main conclusion is that the correction term reinforces the antiferromagnetic character of the ground state in a square and the ferromagnetic one in a triangular lattice. An increase in coercivity of the in-plane systems still cannot be quantitatively explained in the framework of those studies.

Recently, we have calculated explicitly the multipolar (MP) magnetic moments of uniformly and nonuniformly (e.g., onion state) magnetized objects of different symmetry [18,19]. It has been demonstrated that rotationally symmetric particles possess octopolar (Q_3) and dotriacontapolar (Q_5) moments, which can be comparable with the dipolar one (Q_1) for elongated (e.g., nanowires) or ultrathin (e.g., nanodiscs) geometry. The calculation of interaction energies between a pair of particles with multipole moments show, in agreement with [10,12], that the higher-order interactions reinforce the dipolar ones. However, in many-body systems the situation is much more complicated. As it is known from chemistry [20–22] the multipolar interactions may completely change the structure and physical properties of an ensemble. Hence, to make a reliable conclusion about the influence of multipolar interactions on switching behavior stable low-temperature multipolar states have to be calculated. So far, multipolar configurations in magnetic nanoarrays have not been considered despite the small interparticle distances and strong MP moments of the dots or grains.

Few existing calculations of stable MP configurations in physical systems (mainly gas adsorbates) have been usually made within the mean field or Monte Carlo (MC) approach in Cartesian coordinates [22,23]. We use spherical coordinates, as this allows a much easier treatment of higher-order moments and their interaction energies [see Eq. (1) below]. For example, the dotriacontapole has components Q_{5m} with $-5 \leq m \leq 5$ in spherical coordinates while it would be a tensor of the form D_{ijklm} with $(i, j, k, l, m) \in \{x, y, z\}$ in Cartesian coordinates. Even though the number of independent tensor components is the same, it is a formidable task to calculate all components of D_{ijklm} or even higher-order moments. Therefore, the technique, well established in chemical physics, of spherical coordinates is used to calculate the Coulomb interaction energy between two nonintersecting charge distributions [21,24]. A nanoarray is nothing but an ensemble of magnetic multipolar rotators on a lattice and can be described by the extension of this approach onto a many-body MP system.

In this study we introduce the Hamiltonian in spherical coordinates into the conventional MC scheme and derive the stable low-temperature configurations of magnetization as well as hysteretic properties of magnetic nanoarrays. It will be demonstrated that for in-plane systems multipolar interactions select collinear configurations from the dipolar manifold. In patterned media with combined dipolar and octopolar moments a competition between dipole-octopole and dipole-dipole plus octopole-octopole interactions leads to the increase of the coercivity. In out-of-plane systems the higher-order interactions do not change zero-field configurations. However, the multipolar contributions enlarge the interaction field by 10%–15% and, thus, decrease the switching field.

The Hamiltonian of the interaction reads

$$H = \frac{1}{4\pi\mu_0} \sum_{\substack{A \neq B \\ l_A l_B m_A m_B}} T_{l_A l_B m_A m_B}(\vec{R}_{AB}) Q^A_{l_A m_A} Q^B_{l_B m_B} + \sum_A \frac{1}{\sqrt{2}} H_x (Q^A_{11} - Q^A_{1-1}), \quad (1)$$

where $Q^A_{l_A m_A}$ and $Q^B_{l_B m_B}$ are the moments of multipoles A and B expressed in spherical harmonics [18] and $T_{l_A l_B m_A m_B}(\vec{R}_{AB})$ is the geometric interaction tensor depending on the interparticle distance vector $\vec{R}_{AB}$ [21] between multipoles on sites A and B:

$$T_{l_A l_B m_A m_B}(\vec{R}_{AB}) = (-1)^{l_B} I^*_{l_A + l_B m_A + m_B}(\vec{R}_{AB}) \sqrt{\frac{(l_A + l_B - m_A - m_B)!}{(l_A - m_A)!(l_B - m_B)!} \frac{(l_A + l_B + m_A + m_B)!}{(l_A + m_A)!(l_B + m_B)!}}, \quad (2)$$

where the dependency on the distance is given by the complex conjugate of the irregular normalized spherical harmonic function

$$I_{lm}(\vec{r}) = \sqrt{\frac{4\pi}{2l+1}} \frac{Y_{lm}(\theta, \varphi)}{r^{l+1}}. \quad (3)$$

H_x is the only nonvanishing component of an external uniform magnetic field of the form $\vec{H} = (H_x, 0, 0)$.

Two-dimensional films of multipoles or their combinations corresponding to particles of different geometry on a lattice have been considered. In this study we restrict ourselves to rotationally symmetric multipoles with dipolar and octopolar contributions (e.g., Q_{30} or $Q_{30} + Q_{10}$). Rotated moments have components with $m \neq 0$. In the following, the description Q_{l0} means that there exists a coordinate system in which the moments can be represented by Q_{l0}. The weak dotriacontapolar interaction is not presented here as octopolar and dotriacontapolar interactions break the isotropic behavior of dipoles on square and triangular lattices in the same way and the symmetry of the stable magnetic state remains unchanged. Our aim is to give a reasonable theoretical description of finite arrays. For that reason and in order to avoid symmetry adapted structures we use open boundary conditions. Lattice sizes up to 60×60 have been used. To prevent artificial effects we used no cutoff. A standard MC technique was used [3]. The rotational space was sampled uniformly and was not restricted, i.e., a moment can try any new angle. An extremely slow annealing procedure has been applied. To avoid metastable states we have performed two different simulations of the same system simultaneously starting them at different ''seeds'' for the random number generator to ensure that the samples take different path to the equilibrium. Only when both samples reached the same stable energy level it has been deduced that the system has reached equilibrium. The high in-plane coercivity is typically found in assemblies of single domain nanoparticles with a height-to-diameter ratio $h/d \leq 0.5$ [6,8,9,13]. Such particles possess dipole and octopole moments with $Q_{30}/Q_{10} \geq 0.5$ [19]. We have calculated stable configurations for pure octopoles and combined multipoles with $0 \leq Q_{30}/Q_{10} \leq 3.0$. The octopolar moments are unidirectional, i.e., they can be represented as vectors. We find that on the square lattice, octopoles form lines aligned antiparallel while on the triangular lattice the moments are ferromagnetically ordered. Hence, the octopolar interaction on a triangular and a square lattice introduces an easy-plane and a tri- and a biaxial in-plane anisotropy, respectively. In contrast to finite dipolar systems avoiding uncompensated poles by domain formation, a finite octopolar system is not sensitive to the formation of free poles in most geometries as octopoles do not interact with a field but with the field curvature. Therefore the low-temperature configurations in finite samples are still parallel lines for a triangular lattice and antiparallel lines for a square lattice.

With increasing dipolar interaction the pattern changes. A typical low-temperature configuration consists of alter-

nating regions of uniaxial parallel and antiparallel lines such as in Fig. 1(b). On a square lattice the width of regions with parallel lines is usually 2–3 lattice parameters. In ≈ 10% of calculations despite a very long relaxation superdomains [Fig. 1(f)] appear. The energy of ideal and MC configurations as a function of Q_{30}/Q_{10} is plotted in Fig. 2(a). Figure 2(b) gives the size dependence of all energy contributions for parallel lines. We find that the dipole-octopole energy contribution (E_{d-o}) is minimal for the parallel while maximal for the antiparallel lines. The dipole-dipole (E_{d-d}) and octopole-octopole (E_{o-o}) interactions, in contrast, prefer antiparallel lines. Therefore for sample sizes $L < 9$ and $0.25 < Q_{30}/Q_{10} < 0.8$ the state of coexisting parallel and antiparallel lines has the lowest total internal energy. For $L > 9$ the antiparallel lines are preferable for all Q_{30}/Q_{10} as the long-range dipolar contribution increases. The energy difference between antiparallel lines and coexisting phases or superdomains δE grows with increasing Q_{30}/Q_{10} [Fig. 2(a)]. However, for $0 < Q_{30}/Q_{10} < 0.6$ δE is very small (≈2%), while the configurational entropy in a system of parallel or antiparallel lines drastically increases with the system size $S_c = k \ln(2 \times 2^L)$. As the entropy increases boundless with L, in contrast to the slow convergence of the dipolar sum, the free energy of the coexistence is lower for nonzero temperatures.

Formation of superdomains gives an additional contribution to the entropy. The size of superdomains in finite dipolar systems is driven by the pole avoidance principle. While the energy cost due to the wall formation increases only linearly with the domain size, the gain in the long-range dipolar interaction increases with the square of the domain size and only a rare formation of superdomains is observed at low temperatures. The additional entropy for large superdomains is small. Approaching T_c the domain size decreases, the corresponding entropy increases and the superdomains appear more frequently. This finding is in accordance with the experiment [16] giving evidence for formation of the large in-plane collinear domains extending across several dots. At zero temperature the antiparallel lines are preferable.

We have calculated the specific heat $C_v(T, L)$, the order parameter q, and the susceptibility $\chi_q(T, L)$ for different L and Q_{30}/Q_{10}. Using $\beta = (kT)^{-1}$, $C_v(T, L)$ and $\chi_q(T, L)$ are deduced applying the fluctuation-dissipation theorem $C_v = k\beta^2(\langle E^2\rangle - \langle E\rangle^2)$ and $\chi_q = \beta E_{\|}(\langle q^2\rangle - \langle q\rangle^2)$. Figure 3 shows the thermodynamic characteristics in the case of a system with $Q_{30}/Q_{10} = 0.5$. We use $q = N^{-1}|n_x - n_y|$, where $N = n_x + n_y$ is the total number of moments and n_x, n_y number of moments aligned with X or Y directions [15]. All systems show maxima of specific heat and susceptibility at the same temperature confirming the existence of a phase transition. In the following it will be demonstrated that higher-order interactions significantly influence magnetization reversal in nanoarrays.

The field dependence of magnetization in square and triangular arrays of dots with in-plane magnetization and $0 \le Q_{30}/Q_{10} \le 1$ has been calculated. A pure dipolar system does not show any easy-axis hysteresis. In a multipolar array, on the contrary, the hysteresis loop is quite open. The squareness s depends on the composition, the strength of multipoles and on the temperature. Figure 1 shows the magnetization reversal of a square lattice with $Q_{30}/Q_{10} = 0.5$ corresponding to an array of ultrathin particles with $h/d \le 0.5$ [19] and for a pure dipolar system [$h/d \approx 1$, Fig. 1(d)]. The field is scaled with the pair interaction energy $E_{\|}$ between two dots magnetized mutually parallel but perpendicular to the bond $E_{\|} \propto 1/R_{AB}^{l_A+l_B+1}$, therefore, contributions from moments of different order in combined multipoles scale differently with R_{AB}. All

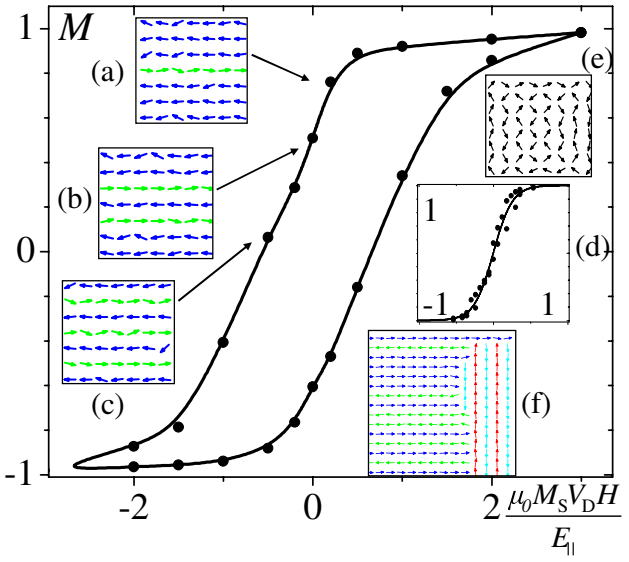

FIG. 1 (color online). Hysteresis loops for a 20×20 square nanoarray with $Q_{30} = 0.5Q_{10}$ and a pure dipolar system [inset (d)]. The magnetic field is applied in the x direction. Insets (a)–(c) give a part of the intermediate magnetic configurations; (f) and (e) show stable zero-field configurations for combined multipoles and the pure dipolar case, respectively. Thermal energy is $kT = 0.6E_{\|}$. The field is expressed in $\frac{\mu_0 M_S V_D}{E_{\|}}$ with μ_0—the permeability of free space and V_D—the volume of a dot.

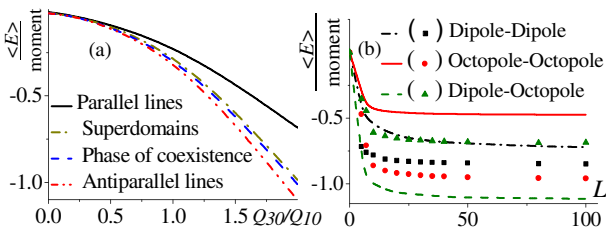

FIG. 2 (color online). (a) Internal energy of ideal parallel, antiparallel, coexisting, and superdomain configurations for $L = 20$ as a function of Q_{30}/Q_{10} on a square lattice; (b) Size dependence of different contributions of the magnetostatic energy for parallel and antiparallel lines (scatter) for $Q_{30}/Q_{10} = 0.5$.

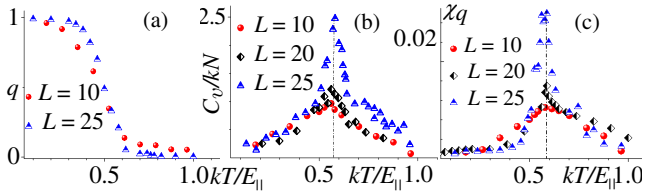

FIG. 3 (color online). MC results for the order parameter (a), specific heat (b), and susceptibility (c) of a system with $Q_{30}/Q_{10} = 0.5$ on a square lattice.

values are given for $Q_3 = 1$, $Q_1 = 2$ and $R_{AB} = 1$. This gives $s \approx 0.5$ and $H_c \mu_0 M_S V_D \approx 0.7 E_{\|}$. By calculating $E_{\|}$ this result can be scaled to a square array of any material with any interdot distance. For example, for an array of permalloy particles at room temperature ($M_S = 8.0 \times 10^5$ A/m and vanishing anisotropy, $K_u < 1000$ J/m^3) with $h = 20$ nm, $d = 70$ nm, and $R = 100$ nm we find $\mu_0 H_c \approx 20$ mT. Magnetic moments do not rotate continuously as in a pure dipolar system but are reoriented line by line [Figs. 1(a)–1(c)] as noncollinear configurations are energetically unfavorable. From our calculations it follows that the competition between the E_{d-o} and $E_{d-d} + E_{o-o}$ interaction energy plays an important role for the magnetization reversal. As has been already demonstrated in Fig. 2(a) the total energy of the configuration Fig. 1(b) is close or even lower than that of Fig. 1(c), where all chains are antiparallel. Hence, to go from configuration Fig. 1(b) to the configuration Fig. 1(c), an external magnetic field has to be applied and the hysteresis appears. H_c increases with decreasing temperature. This effect is similar to the superparamagnetic temperature assisted switching. Thus, the hysteretic behavior is predefined by the competition between the octopole-dipole contribution of the magnetostatic energy and its dipole-dipole and octopole-octopole counterparts. Pure dipolar systems do not show any significant hysteresis.

On a triangular lattice H_c increases by ≈10% compared to the pure dipolar system in good accordance with experiments [6]. The increase is due to the support of the ferromagnetic single domain state by all interactions. For assemblies of single domain nanoparticles with out-of-plane magnetization [7] multipolar contributions do not change the ground states of a dipolar system (checkerboard pattern on a square and labyrinthine structure on a triangular lattice). They give, however, an additional energetic contribution promoting the magnetization reversal. Thus, one of the main reasons for increase (decrease) of coercivity in the in-plane (out-of-plane) magnetic nanoarrays are multipolar energetic contributions. In addition, the octopole-dipole interaction between magnetic grains of ultrathin geometry with in-plane magnetization might explain the origin and stability of superferromagnetic domains in magnetostatically coupled nanosystems [9,17].

In conclusion, systematic investigation of multipolar low-temperature stable configurations on a triangular and a square lattice have been carried out theoretically. In contrast to previous results we demonstrate that the MP-MP interactions change considerably stable low-temperature dipolar states. The dipole-octopole interaction is an important component that might also explain the superferromagnetic behavior in dense grain magnetic materials and magnetic arrays. Tuning the multipole moments by changing the geometry of nanoparticles offers a new route to the control of the coupling behavior and therefore the hysteretic properties of magnetic nanoparticle arrays.

Financial support from the Interdisciplinary Nanoscience Center Hamburg (INCH) is gratefully acknowledged.

[1] S. P. Li, W. S. Lew, J. A. C. Bland, L. Lopez-Diaz, M. Natali, C. A. F. Vaz, and Y. Chen, Nature (London) **415**, 600 (2002).
[2] T. Aign *et al.*, Phys. Rev. Lett. **81**, 5656 (1998).
[3] E. Y. Vedmedenko, A. Kubetzka, K. von Bergmann, O. Pietzsch, M. Bode, H. P. Oepen, and J. Kirschner, Phys. Rev. Lett. **92**, 077207 (2004).
[4] R. P. Cowburn and M. E. Welland, Science **287**, 1466 (2000).
[5] C. A. Ross *et al.*, Phys. Rev. B **65**, 144417 (2002).
[6] J. Y. Cheng, W. Jung, and C. A. Ross, Phys. Rev. B **70**, 064417 (2004).
[7] K. Nielsch *et al.*, J. Magn. Magn. Mater. **249**, 234 (2002).
[8] R. P. Cowburn, J. Phys. D **33**, R1 (2000).
[9] M. R. Scheinfein, K. E. Schmidt, K. R. Heim, and G. Hembree, Phys. Rev. Lett. **76**, 1541 (1996).
[10] P. Politi and M. G. Pini, Phys. Rev. B **66**, 214414 (2002).
[11] A. J. Bennett and J. M. Xu, Appl. Phys. Lett. **82**, 2503 (2003).
[12] P. J. Jensen and G. M. Pastor, New J. Phys. **5**, 68 (2003).
[13] C. Miramond, C. Fermon, F. Rousseaux, D. Decanini, and F. Carcenac, J. Magn. Magn. Mater. **165**, 500 (1997).
[14] K. Y. Guslienko, Appl. Phys. Lett. **75**, 394 (1999).
[15] E. Olive and P. Molho, Phys. Rev. B **58**, 9238 (1998).
[16] Y. B. Xu *et al.*, IEEE Trans. Magn. **37**, 2055 (2001).
[17] W. Kleemann, O. Petracic, C. Binek, G. N. Kakazei, Y. G. Pogorelov, J. Sousa, S. Cardoso, and P. P. Freitas, Phys. Rev. B **63**, 134423 (2001).
[18] N. Mikuszeit, E. Y. Vedmedenko, and H. Oepen, J. Phys. Condens. Matter **16**, 9037 (2004).
[19] N. Mikuszeit, E. Y. Vedmedenko, R. Wiesendanger, and H. P. Oepen, J. Appl. Phys. **97**, 10J502 (2005).
[20] M. Eremtchenko, J. A. Schaefer, and F. S. Tautz, Nature (London) **425**, 602 (2003).
[21] P. Popelier and D. Kosov, J. Chem. Phys. **114**, 6539 (2001).
[22] A. J. Berlinsky and A. B. Harris, Phys. Rev. Lett. **40**, 1579 (1978).
[23] V. E. Klymenko, V. M. Rozenbaum, V. V. Kukhtin, and O. V. Schramko, Solid State Commun. **88**, 373 (1993).
[24] S. F. O'Shea, J. Chem. Phys. **71**, 2399 (1979).